Progress In Electromagnetics Research, Vol. 106, 49–60, 2010

COMPACT TRI-LAYER ULTRA-WIDEBAND BAND-PASS FILTER WITH DUAL NOTCH BANDS

P.-Y. Hsiao and R.-M. Weng

Department of Electrical Engineering
National Dong Hwa University
Hualien, Taiwan, R.O.C.

Abstract—A compact ultra-wideband (UWB) bandpass filter (BPF) with dual notch bands is presented using a tri-layer structure. In the design of UWB BPFs, it is desired to have a uniform 3.1 GHz to 10.6 GHz full-band transmission response. Dual notch bands are generated for filtering out the interferences caused by strong signals transmitted from WLAN and/or WiMAX systems at 5.8 GHz and 3.5 GHz, respectively. The sharp rejection of WiMAX signals is achieved by adding meander open-loop resonators on the middle layer. Another rejection of WLAN signals is introduced by adding a C-shaped resonator on the bottom layer. The proposed filter is not only realized theoretically but also verified by a full-wave electromagnetic simulation. The designed tri-layer UWB BPF with dual notch bands was fabricated by two FR4 printed circuit boards with the permittivity of 4.4 and the thickness of 0.8 mm. The total area is 11 mm × 10.5 mm.

1. INTRODUCTION

Ultra-wideband (UWB) systems enable personal area network wireless connectivity since the Federal Communications Commission (FCC) released the frequency band from 3.1 to 10.6 GHz for high data rate communication in 2002 [1]. UWB bandpass filters (BPFs) used in UWB receivers are implemented by microwave passive elements [2–8]. BPFs are presented for filtering out unwanted signals besides UWB frequency spectrum [9–11]. Most UWB BPFs suffered from narrow upper-stopband and large overall sizes. Previously, a wide upper-stopband using a detached-mode resonator composed of a quarter-wave-length nonuniform coplanar waveguide (CPW) resonator within

Received 2 April 2010, Accepted 30 June 2010, Scheduled 9 July 2010
Corresponding author: P.-Y. Hsiao (d9523008@ems.ndhu.edu.tw).

11.4 to 16.4 GHz with a notch band was observed [12]. However, a large size is inevitable using CPW resonators. Investigation in open-circuit metal lines embedded in defected ground structures (DGSs) behaves simple for UWB BPF with a notch band [13]. UWB BPFs with multi notch bands become important when wireless communication systems are coexisting with UWB systems. Dual notch bands embedded in UWB BPFs can avoid interferences to UWB systems from other radio systems (5.6 GHz/6.48 GHz) [14]. A compact UWB filter with dual notch bands using stepped impedance resonators (SIRs) was designed to suppress out-of-band harmonic response. A broadside-coupled technique was adopted to realize wideband tight coupling [15]. UWB BPF using short-circuit stubs in the first connecting line along with open-circuit stubs in the last connecting line was presented to reject the undesired signals from WLAN systems [16]. An alternative design of filter combined a conventional bandpass characteristic and a negative permittivity meta-material to establish UWB response and extra wave propagation to reject the interference [17]. A pair of shunt and open-stubs was embedded to obtain both sharp rejection and wide stopband [18]. A multi-mode resonator (MMR)-based band-notched UWB BPF with an improved upper stopband was designed and verified [19]. However, those filters consume large sizes. Tri-layer structures were adopted to minimize the sizes of UWB BPFs. A complicated C-shaped structure was proposed for a small UWB BPF with WLAN notch band [20]. Two pairs of open-loop resonators on the top layer and one coupled resonator on the bottom layer was proposed [21] The size reduction can be achieved successfully by tri-layer structure. Commonly, possible interferences within the allocated UWB spectrum are caused by relatively strong narrowband signals transmitted from WLAN systems at 5.8 GHz and/or worldwide interoperability for microwave access (WiMAX) systems at 3.5 GHz. Hence, it is desirable for microwave filter designers to implement UWB BPFs with dual notch bands. This paper presents a compact UWB BPF with dual notch bands to avoid interferences from WLAN systems at 5.8 GHz and WiMAX systems at 3.5 GHz.

2. DESIGN OF UWB FILTER WITH DUAL NOTCH BANDS

Figure 1 illustrates the configuration of the proposed UWB BPF with dual notch bands. A tri-layer technique is adopted to achieve a compact size. Two open-loop microstrip line resonators are implemented on the top layer. Two meanders open-loop resonators are added on the middle layer. For the purpose of compact sizes,

DGSs are commonly adopted. One C-shaped resonator using DGS is designed on the bottom layer.

The input/output feed lines with 1.47 mm width are designed to match 50 Ω, the characteristic impedance of a microstrip line. The open-loop microstrip line on the top layer and the coupled C-shaped DGS on the bottom layer generates the notch band at 5.8 GHz, whereas the embedded meander open-loop resonators on the middle layer and

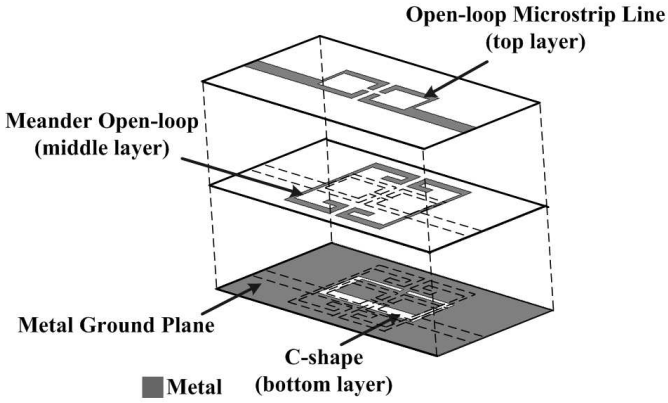

Figure 1. Proposed UWB BPF with dual notch bands.

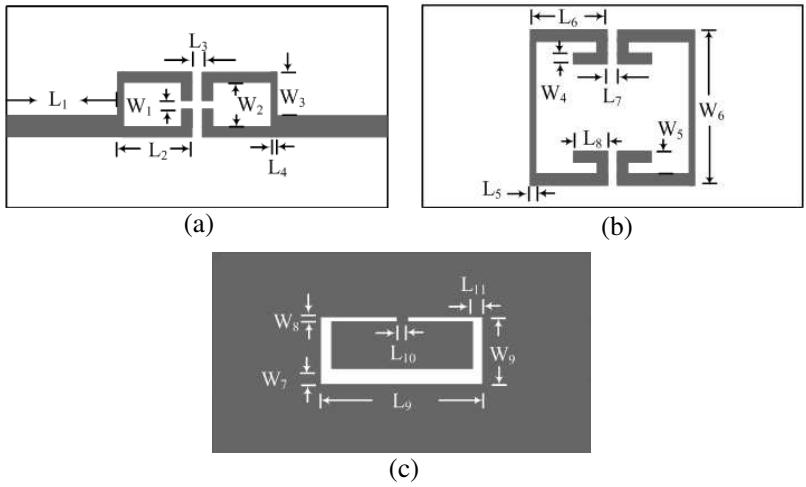

Figure 2. Schematics of the proposed UWB BPF with dual notch bands. (a) The top layer, (b) the middle layer, and (c) the bottom layer.

the coupled C-shaped DGS on the bottom layer creates the 3.5 GHz notch band. Figs. 2(a), (b), and (c) show the patterns and size denotation of the top layer, the middle layer, and the bottom layer of the filter, respectively.

3. SIMULATION RESULTS

The design concept is illustrated by a full-wave electromagnetic (EM) simulator. Fig. 3 depicts the EM simulation of the insertion loss $|S_{21}|$ to show the generation of the dual notch bands. As depicted in Fig. 3, the first notch band in the lower frequency band can be generated by embedding two meander open-loop resonators on the middle layer and loading the C-shaped resonator closely coupled. The WiMAX interference to UWB systems is filtered out by the first notch band. The second notch band in the higher frequency band is created by adding an open-loop microstrip line on the top layer and loading the C-shaped resonator closely coupled. The WLAN interference to UWB systems is filtered out by the second notch band.

Figure 4 shows the current density distribution on the top layer as well as the middle layer operated at dual notch bands. It can be observed from Fig. 4(a) that the width W_6 distributes a maximum current at 3.5 GHz on the middle layer. A minimum current density occurs at the end of the length L_8 and the width W_4. At the second notch band of 5.8 GHz, maximum current density is shown obviously in the length L_2 and the width W_3 as illustrated in Fig. 4(b).

Figure 5(a) shows the transmission response of the modified meander open-loop resonators with different coupled lengths. When

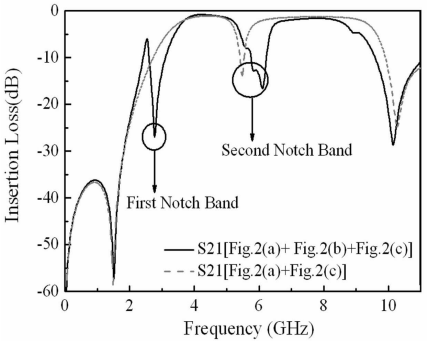

Figure 3. Full-wave EM simulation of $|S_{21}|$.

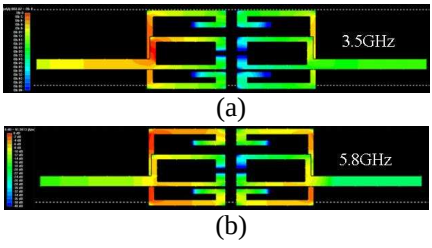

Figure 4. Current distribution at (a) 3.5 GHz, and (b) 5.8 GHz.

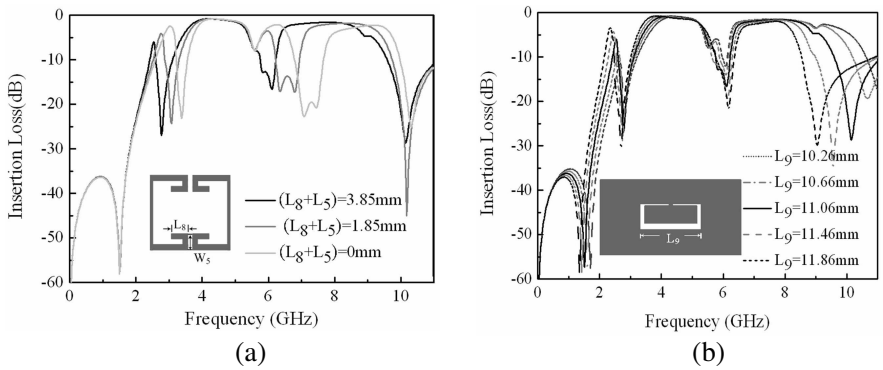

Figure 5. Full-wave EM simulation of adjusting the sizes of patterns on (a) the middle layer and (b) the bottom layer.

the total length of L_8 and L_5 equals to 3.85 mm, the transmission zeros of $|S_{21}|$ are -57.05 dB at 1.5 GHz and -28.71 dB at 10.2 GHz. However, none of the dual notch bands for these cases are wide enough to cover the bandwidth for WiMAX and WLAN. It is obviously that the dual notch bands are shifted to high frequencies while reducing the total length of L_8 and L_5 of the open-loop resonators on the middle layer.

C-shaped resonator is a defect-grounded pattern on the bottom layer for the compact reason. The signal coupling can be varied to control the bandwidth. That is, the bandwidth of the notch band can be controlled by proper selection of the circuit parameters of the C-shaped resonator. Fig. 5(b) shows that the bandwidth of the UWB passband can be modified by adjusting L_9, the length of the C-shaped slot. The fractional bandwidths (FBW) which are calculated by the ratio of the bandwidth to the center frequency are among 104% to134% after varying L_9.

Figure 6 show the equivalent circuit model of the propsoed bandpass filter with dual notch bands. The passive element values of the equivalent lumped circuit can be easily obtained by curve-fitting method from the simulation results. Each part of the equivalent circuit was simulated separately using an Ansoft simulator. The data were fitted into the circuit model to derive the appropriate passive element values.

The symmetric open-loop resonators on the top layer can be modeled by two LC resonators. The resonator on each side includes a capacitor C_a, an inductor L_a, and a resistor R_a in series with a coupling capacitor C_b. R_a is the effect of the dielectric loss of the material.

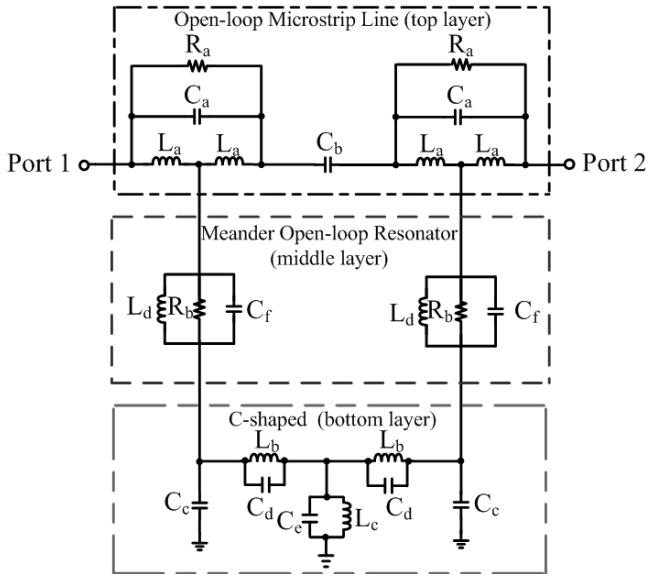

Figure 6. Equivalent circuit of UWB BPF with dual notch-bands.

Table 1. Components of the equivalent circuit (L: nH, C: pF, R: kΩ)).

L_a	L_b	L_c	L_d	C_a	C_b	C_c	C_d	C_e	C_f	R_a	R_b
0.075	1	0.1	0.19	1.7	1.3	0.5	0.1	8	22	100	20

Relative large insertion loss is generated at high frequency due to the coupling capacitor between two openloop resonators. The C-shaped slot produces two pairs of inductor L_b and capacitor C_d associated with the enclosure, which creates a ground capacitor C_c. L_b and C_d represent the characteristics of the planar C-shaped slot on the bottom layer. Two pairs of LC resonators, L_d, C_f, and R_b, are shunted to be equivalent to the meander open-loop resonators on the middle layer to form the first notch band. L_c and C_e which are related to the mutual coupling between the open-loop resonators on the top layer and C-shaped slot on the bottom layer are shunted to generate the second notch band. The passive component values of the equivalent lumped circuit are listed in Table 1.

Following the approach outlined in the preceding section, a prototype of the proposed 3.5 GHz and 5.8 GHz dual band-notched UWB BPF was fabricated and measured for the performance

demonstration. The feature of the proposed structure is simulated in prior to its fabrication. The dimensions of the prototype UWB BPF with dual notch bands are $L_1 = 7.5$, $L_2 = 5$, $L_3 = 0.7$, $L_4 = 0.4$, $L_5 = 0.4$, $L_6 = 5.25$, $L_7 = 0.7$, $L_8 = 2.3$, $L_9 = 11.06$, $L_{10} = 0.7$, $L_{11} = 0.8$, $W_1 = 0.5$, $W_2 = 3$, $W_3 = 2.93$, $W_4 = 0.75$, $W_5 = 1.5$, $W_6 = 10.5$, $W_7 = 1.2$, $W_8 = 0.4$, $W_9 = 4.75$. All dimensions are in the units of mm.

Figure 7 shows the similarity between the circuit model simulation and the EM simulation results of the proposed UWB BPF. It is obvious that UWB at 2.6 GHz–9.6 GHz are formed by the tri-layer structure. When meander open-loop resonators on the middle layer are introduced, the first notch band at 3.5 GHz is excited. When the C-shaped resonator on the bottom layer is introduced, the second notch band at 5.8 GHz is excited. Using tri-layer structure can achieve dual notch bands which prevent the interference caused by the signals from adjacent WiMAX and WLAN systems.

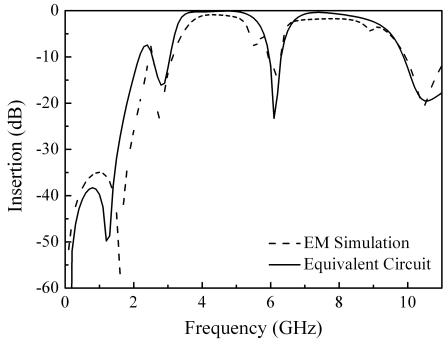

Figure 7. Circuit model simulation and EM simulation results.

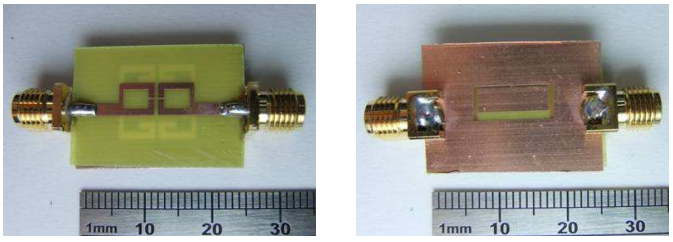

(a) (b)

Figure 8. Realization of the UWB BPF with dual notch bands. (a) Top view, and (b) bottom view.

4. MEASUREMENT RESULTS

Microstrip substrates with a relative dielectric constant of 4.4 and a thickness of 0.8 mm using the printed circuit board (PCB) technology are low cost and commonly adopted in the fabrication of microwave filters. The proposed UWB filter is fabricated using two FR4 boards with 0.4 mm thickness of each board. A thin FR4-G11 epoxy glass fiber board with 0.1 mm thickness as an insulating material is inserted between two FR4 boards. These three boards are further bonded by a multi-layer lamination machine. Since an air-gap problem is existed using such fabrication technology, insertion loss at high frequency operation band is inevitable. The total thickness is 0.8 mm, which composes copper layers on the top, the middle, and the bottom layers. The input and output feed lines are placed on the top layer. Since the implementation of the embedded stubs does not enlarge the filter size, the fabricated filter with tri-layer structure has the same size of 11 mm × 10.5 mm as that of UWB systems on the substrate. The fabricated filter on PCB attaching SMA connectors is photographed and shown in Fig. 8.

Asymmetric meander open-loop resonators on the middle layer are added to reject the undesired WiMAX signals. Fig. 9 depicts the insertion of 3.5 GHz notch band by adding the meander open-loop resonators.

The EM simulation and the measurement results of the UWB filter are depicted in Fig. 10. It can be seen that the filter exhibits an excellent UWB bandpass performance with fractional bandwidth (FBW) of 120%. The measured 3 dB bandwidth for UWB filter is within 2.6 GHz to 9.6 GHz. In the first notch band of 3.5 GHz, $|S_{11}|$

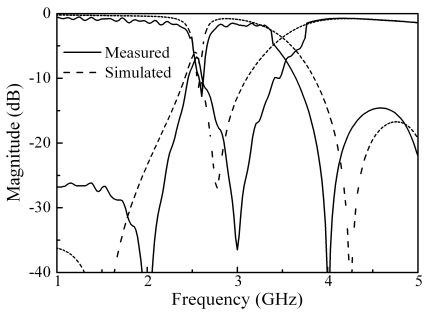

Figure 9. Simulated and measured results of 3.5 GHz notch insertion.

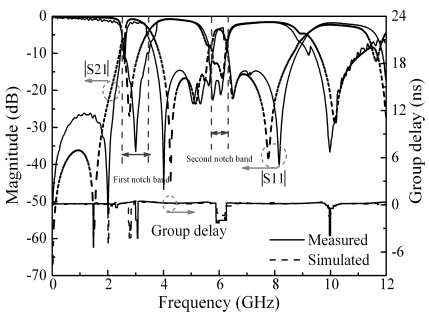

Figure 10. Simulated and measured results.

Table 2. Specifications of the proposed UWB BPF with dual notch bands.

Spec.	UWB (GHz)	Notch (GHz)	Notch (GHz)	Group Delay (ns)
Simulated	2.6–9.6	3.5	5.8	0.3
Measured	2.6–9.5	3.5	5.8	0.3

Table 3. Comparison of various UWB BPFs.

Parameters \Ref.	[16] 2008	[17] 2008	[18] 2009	[19] 2008	[20] 2009	[21] 2010	This work
Permittivity	10.8	2.2	2.2	10.2	4.4	4.4	4.4
Thickness (mm)	1.27	0.787	0.508	0.635	0.8	0.8	0.8
Loss Tangent	0.0023	0.0023	0.0027	0.0023	0.0245	0.0245	0.0245
Pass band (GHz)	2.8–10.8	3.1–10.6	3.1–9.7	3.1–10.6	3.1–10.6	3.1–10.6	2.6–9.6
Notch band	5.47	5.4	5.5	5.5	5.75	5.75	3.5/5.8
Transmission zeros	Two	None	Two	None	Two	Two	Four
Etched size (mm^2)	36×16	45×11	25×25	25.4×6.48	21×12	20×5.7	11×10.5
Relative Size	4.9	4.2	5.4	1.43	2.04	0.97	1

and $|S_{21}|$ are -1.77 dB and -28.3 dB, respectively. The measured 3 dB bandwidths and FBW of the first notched band are 2.43.5 GHz and 45.8%, respectively. Since the first notch band is close to 3.1 GHz, the low frequency bandwidth limitation of UWB systems, the first notch band cause possibly the degradation of the in-band performance for the lower passband. Consequently, a sharp rejection notch band is required at 3.5 GHz. In the second notch band of 5.8 GHz, $|S_{11}|$ and $|S_{21}|$ are -20.8 dB and -3.06 dB, respectively. The measured 3 dB bandwidth and FBW for the second notch band is 5.85–6.15 GHz and 5%, respectively. The filter performs a flat group delay less than 0.3ns at the center frequency of each passband. As shown in Fig. 10, the problem of air-gap in tri-lay structure causes inevitable insertion loss at high frequency operation band. The specifications of both simulated and measured results are listed in Table 2. The performance of the proposed filter along with the parameters of other

UWB BPFs with only one notch band in the previous publication are compared in Table 3. The results show that the presented UWB BPF with dual notch bands using tri-layer structure has the advantage of miniaturization.

5. CONCLUSION

A tri-layer coupling structure for dual notch bands implementation in UWB bandpass filter has been developed and presented. The new technique for generating two notch bands is based on adding an extra the middle layer between the top microstrip layer and the bottom ground layer. The proposed filter not only provides a coupling effect over an ultra-wide passband but also introduces dual notch bands within the passband. The dual notch bands can be controlled properly by adjusting the parameters of the meander open-loop resonators on the middle layer and C-shaped slot on the bottom layer for interferences transmitted from WiMAX sand WLAN systems, respectively. The filter performs a flat group delay at the center frequency of each passband. Furthermore, the designed filter can be implemented using multiple-layer microstrip line structure on FR4 substrates for low cost, easy integration, and simple fabrication. A good agreement between the simulated and the measured results is obtained. Therefore, the proposed UWB BPF with dual notch bands is promising for the use in the UWB wireless communication systems to provide an efficient method for solving the problem of WiMAX and WLAN interferences allocated in the UWB spectrum.

REFERENCES

1. FCC, Revision of Part 15, the Commission's Rules Regarding to Ultra-Wide-Band Transmission System, First Note and Order Federal Communication Commission, ET-Docket 98-153, 2002.
2. Chen, H. and Y.-X. Zhang, "A novel and compact UWB bandpass filter using microstrip fork-form resonators," *Progress In Electromagnetics Research*, Vol. 77, 273–280, 2007.
3. Gao, S. S., X. S. Yang, J. P. Wang, S. Q. Xiao, and B. Z. Wang, "Compact ultra-wideband (UWB) bandpass filter using modified stepped impedance resonator," *Journal of Electromagnetic Waves and Applications*, Vol. 22, No. 4, 541–548, 2008.
4. Gong, J.-Q. and Q.-X. Chu, "SCRLH TL based UWB bandpass filter with widened upper stopband," *Journal of Electromagnetic Waves and Applications*, Vol. 22, Nos. 14–15, 1985–1992, 2008.

5. Qiang, L., Y.-J. Zhao, Q. Sun, W. Zhao, and B. Liu, "A compact UWB bandpass filter based on complementary split-ring resonators," *Progress In Electromagnetics Research C*, Vol. 11, 237–243, 2009.
6. Packiaraj, D., K. J. Vinoy, and A. T. Kalghatgi, "Analysis and design of two layered ultra wide band filter," *Journal of Electromagnetic Waves and Applications*, Vol. 23, Nos. 8–9, 1235–1243, 2009.
7. Razalli, M. S., A. Ismail, M. A. Mahdi, and M. N. Hamidon, "Via-less UWB filter using patched microstrip stubs," *Journal of Electromagnetic Waves and Applications*, Vol. 23, Nos. 2–3, 377–388, 2009.
8. Tang, I.-T., D.-B. Lin, C.-M. Li, and M.-Y. Chiu, "Compact pentagon ultra-wideband band-pass filter with good out-of-band performance," *Journal of Electromagnetic Waves and Applications*, Vol. 23, 1695–1706, No. 13, 2009.
9. NaghshvarianJahromi, M. and M. Tayarani, "Miniature planar UWB bandpass filters with circular slots in ground," *Progress In Electromagnetics Research Letters*, Vol. 3, 87–93, 2008.
10. An, J., G.-M. Wang, W.-D. Zeng, and L.-X. Ma, "UWB filter using defected ground structure of von koch fractal shape slot," *Progress In Electromagnetics Research Letters*, Vol. 6, 61–66, 2009.
11. Wei, F., L. Chen, X.-W. Shi, X. H. Wang, and Q. Huang, "Compact UWB bandpass filter with notched band," *Progress In Electromagnetics Research C*, Vol. 4, 121–128, 2008.
12. Hao, Z.-C. and J.-S. Hong, "Compact UWB filter with double notch-bands using multilayer LCP technology," *IEEE Microwave Compon. Lett.*, Vol. 19, No. 8, 500–502, Aug. 2009.
13. Luo, X., J.-G. Ma, K. Ma, and K.-S. Yeo, "Compact UWB bandpass filter with ultra narrow notched band," *IEEE Microwave Compon. Lett.*, Vol. 20, No. 3, 145–147, Mar. 2010.
14. Li, K., K. Daisuke, and T. Matsui, "UWB bandpass filters with multi notched bands," *36th European Microwave Conference*, 591–594, 2006.
15. Lin, W.-J., J.-Y. Li, L.-S. Chen, D.-B. Lin, and M.-P. Houng, "Investigation in open circuited metal lines embedded in defected ground structure and its applications to UWB filters," *IEEE Microwave Compon. Lett.*, Vol. 20, No. 3, 148–150, Mar. 2010.
16. Yang, G.-M., R. Jin, C. Vittoria, V. G. Harris, and N. X. Sun, "Small ultra-wideband (UWB) bandpass filter with notched band," *IEEE Microwave Compon. Lett.*, Vol. 18, No. 3, 176–178,

2008.

17. Ali, A. and Z. Hu, "Metamaterial resonator based wave propagation notch for ultrawideband filter applications," *IEEE Antennas Wireless Propag. Lett.*, Vol. 7, 210–212, Sep. 2008.
18. Weng, M.-H., H. Kuan, W.-L. Chen, C.-S. Ye, and Y.-K. Su, "Design of a stopband-improved UWB filter using a pair of shunt and embedded open stubs," *Microwave and Optical Technology Letters*, Vol. 51, No. 9, 2121–2124, Sep. 2009.
19. Lee, C.-H., I.-C. Wang, and L.-Y. Chen, "MMR-based band-notched UWB bandpass filter design," *Journal of Electromagnetic Waves and Applications*, Vol. 22, Nos. 17–18, 2407–2415, 2008.
20. Hsiao, P.-Y. and R.-M. Weng, "Compact open-loop UWB filter with notched band," *Progress In Electromagnetics Research Letters*, Vol. 7, 149–159, 2009.
21. Hsiao, P.-Y. and R.-M. Weng, "C-shaped ultra-wideband bandpass filter with WLAN notch band," *Microwave and Optical Technology Letters*, Vol. 52, No. 5, 1215–1218, May 2010.